10x GENOMICS

Single Cell and Spatial Technologies to Advance Your Research

Resolve highly complex biological systems, while bringing into focus the details that matter most. Explore biology at true resolution.

Join the conversation with exclusive live talks at Europe-friendly times, or enjoy on-demand recordings at your leisure!

Join the Conversation

Together we succeed!

Get a sneak peek into the progress we're making as a community to optimize single cell and spatial transcriptomics workflows at every step.

10x Genomics & Illumina Coffee-Break Conversations

Learn how single cell sequencing and spatial transcriptomics can unlock biological mysteries across a number of research areas.

10x Genomics European Virtual Scientific Symposium

Learn how single cell and spatial technologies are driving fundamental discoveries across multiple areas of biology, including cancer, immunology, neuroscience—and COVID-19.

And more...

RESEARCH REPORT

Loss of the psychiatric risk factor SLC6A15 is associated with increased metabolic functions in primary hippocampal neurons

Karla-Gerlinde Schraut[1] | Oleksandra Kalnytska[1] | Daniel Lamp[2] | Martin Jastroch[2] |
Matthias Eder[3] | Felix Hausch[4] | Nils C. Gassen[5] | Sarah Moore[6,7] |
Nagarjuna Nagaraj[8] | Juan P. Lopez[3] | Alon Chen[3] [iD] | Mathias V. Schmidt[1] [iD]

[1]Research Group Neurobiology of Stress Resilience, Max Planck Institute of Psychiatry, Munich, Germany

[2]Institute for Diabetes and Obesity, Helmholtz Zentrum München, Neuherberg, Germany

[3]Department Stress Neurobiology and Neurogenetics, Max Planck Institute of Psychiatry, Munich, Germany

[4]Structure-Based Drug Research, Technische Universität Darmstadt, Darmstadt, Germany

[5]Department of Psychiatry and Psychotherapy, Bonn Clinical Center, University of Bonn, Bonn, Germany

[6]Department of Medical Genetics, University of British Columbia, BC Children's Hospital Research Institute, Vancouver, Canada

[7]Department Translational Psychiatry, Max Planck Institute of Psychiatry, Munich, Germany

[8]Biochemistry Core Facility, Max Planck Institute of Biochemistry, Munich, Germany

Correspondence
Mathias V. Schmidt, Research Group Neurobiology of Stress Resilience, Max Planck Institute of Psychiatry, Kraepelinstr. 2-10, 80804 Munich, Germany.
Email: mschmidt@psych.mpg.de

Funding information
Max Planck Innovations

Abstract

Major depressive disorder (MDD) is one of the most severe global health problems with millions of people affected, however, the mechanisms underlying this disorder is still poorly understood. Genome-wide association studies have highlighted a link between the neutral amino acid transporter SLC6A15 and MDD. Additionally, a number of preclinical studies support the function of this transporter in modulating levels of brain neurotransmitters, stress system regulation and behavioural phenotypes related to MDD. However, the molecular and functional mechanisms involved in this interaction are still unresolved. Therefore, to investigate the effects of the SLC6A15 transporter, we used hippocampal tissue from *Slc6a15*-KO and wild-type mice, together with several in-vitro assays in primary hippocampal neurons. Utilizing a proteomics approach we identified differentially regulated proteins that formed a regulatory network and pathway analysis indicated significantly affected cellular domains, including metabolic, mitochondrial and structural functions. Furthermore, we observed reduced release probability at glutamatergic synapses, increased mitochondrial function, higher GSH/GSSG redox ratio and an improved neurite outgrowth in primary neurons lacking SLC6A15. In summary, we hypothesize that by controlling the intracellular concentrations of neutral amino acids, SLC6A15 affects mitochondrial activity, which could lead to alterations in neuronal structure and activity. These data provide further indication that a pharmacological or genetic reduction of SLC6A15 activity may indeed be a promising approach for antidepressant therapy.

KEYWORDS

amino acid transport, cell metabolism, depression, proline, SLC6A15

Edited by Prof. Tamas Kozicz

1 | INTRODUCTION

According to the World Health Organization (WHO), major depressive disorder (MDD) is the leading cause of disability, with more than 300 million people suffering worldwide (James et al., 2018; Wittchen et al., 2011). While pharmacological and non-pharmacological treatments exist, many patients remain unresponsive to medication, there is a high relapse rate in those initially successfully treated (Schumann et al., 2014), and the medication often has significant side effects. These shortcomings in MDD treatment partly result from our lack of understanding of the molecular and cellular processes that transmit the intricate interaction of genetic and environmental risk factors and illustrate the urgent need for research in this field.

In the vast wake of genome-wide association studies (GWAS) and meta-analysis studies trying to pinpoint genetic risk factors for psychiatric disorders, *SLC6A15* has recently gained attention due to several publications implicating the gene in the etiology of MDD. Single nucleotide polymorphisms (SNPs) near *SLC6A15* correlated with MDD prevalence and stress vulnerability (Kohli et al., 2011), and hypothalamus-pituitary-adrenal (HPA) axis regulation and memory (Schuhmacher et al., 2013). Recently, another SNP in close proximity to *SLC6A15* reached genome-wide significance in a joint study that associated 15 genetic loci with the risk of MDD (Hyde et al., 2016).

SLC6A15 (also referred to as B(0)AT2 or v7-3) is a member of the well-known solute carrier 6 protein family, the more prominent members being the serotonin transporter (SLC6A4) and the norepinephrine transporter (SLC6A2). The protein encoded by *SLC6A15* is a sodium-dependent symporter for neutral amino-acids, with the major substrates being proline, the essential branched amino acids leucine and isoleucine, and the methyl donor methionine (O'Mara et al., 2006; Takanaga et al., 2005). It is expressed in a small percentage of neurons in the hippocampus, the amygdala and other limbic regions (Zeisel et al., 2015), as well as in the olfactory bulb, the cortex and the cerebellum (Farmer et al., 2000; Inoue et al., 1996). Despite the transporter's highly abundant substrates and restricted expression, a complete ablation of the gene in mice reduces leucine and proline uptake into cortical synaptosomes by 40% and 15%, respectively (Drgonova et al., 2007). Furthermore, ablation reduces the overall tissue content of its substrates in the hippocampus, but also tissue glutamate and GABA levels in hippocampus and prefrontal cortex (PFC; Santarelli et al., 2015, 2016). Moreover, behavioural studies have implicated this gene in coping with stress: knock-out (KO) mice show increased baseline corticosterone levels, but also a stronger downregulation of corticosterone (CORT) 90 min after acute stress, and an increased latency to float in the forced swim test as compared to wild-type (WT) mice (Santarelli et al., 2016). Chandra and colleagues down-regulated SLC6A15-levels in D2-neurons of the nucleus accumbens of mice and found an increased susceptibility to subthreshold social defeat stress in the social interaction test, while restoration of SLC6A15 expression rescued normal behaviour (Chandra et al., 2017).

Although there is converging evidence that SLC6A15 expression impacts brain chemistry and mouse behaviour, the underlying mechanisms are as yet obscure. Possible modes of action comprise a direct effect of the altered proline availability on glutamate synthesis, metabolic effects of altered essential branched amino acid levels, e.g., via the mTOR pathway, and epigenetic effects due to the reduced abundancy of methionine-derived methyl groups. Therefore, we first used proteomics on tissue extract of the mouse hippocampus, the major site of SLC6A15 expression in the mouse brain, to get an indication of pathways affected by a KO of *Slc6a15* and then followed up on different cellular functions associated with substrates of the transporter as well as glutamate in primary neurons, i.e., electrophysiology, oxidative phosphorylation, redox state and neurite outgrowth. We found that SLC6A15 KO leads to reduced frequency of AMPA-mediated mEPSCs, whereas cell metabolism and neurite outgrowth were increased.

2 | MATERIALS AND METHODS

2.1 | Animals

All the procedures involving animals were carried out according to the European Communities Council Directive 2010/63/EU and approved by the committee for the Care and Use of Laboratory Animals of the Government of Upper Bavaria, Germany. *Slc6a15*-KO mice on C57BL/6J background were kindly provided (Drgonova et al., 2007) and kept as in house colony at standard housing conditions including chow and water ad libitum. Animals for proteomics were generated from heterozygous breeding pairs, while embryos for primary cell culture were generated from homozygous breeding pairs.

2.2 | Proteomics

Protein expression profiles were generated using whole proteome analysis on dorsal hippocampi extracted from adult (3–6 month old) male *Slc6a15*-KO and WT mice ($n = 3$–5 per group).

2.2.1 | Sample preparation

Tissues were homogenized in a lysis buffer containing 1% sodium deoxycholate, 10 mM TCEP and 40 mM

chloroacetamide in 25 mM Tris, pH 8.5. Homogenized samples were heated at 95°C for 2 min. Samples were diluted onefold with water and digested at 37°C using endoproteinase lysC (Wako Pure Chemicals, Fujifilm) for two hours. Subsequently, the samples were further digested using trypsin (Promega) overnight. Digested peptides were purified using StageTips (Rappsilber et al., 2003).

2.2.2 | Liquid chromatography mass spectrometry

Peptides were loaded on an in-house packed column (50 cm long, 75 μm inner diameter packed with 1.9 μm C18 beads from Reprosil) using the autosampler of Easy nLC 1200 (Thermo Scientific) and sprayed directly into Q Exactive HF mass spectrometer (Thermo Scientific). The mass spectrometer was operated in a data dependent mode with up to Top15 precursors (Nagaraj et al., 2012) were selected for fragmentation by HCD.

2.2.3 | Data analysis

Raw data were processed in MaxQuant (Cox & Mann, 2008) computational software version 1.6.0.15 and protein and peptide identification were filtered at 1% false discovery rate. Match between the runs feature was enabled and MaxLFQ algorithm (Cox et al., 2014) was used for protein quantification. Candidate proteins and the remaining whole proteome data ($n = 6,404$ proteins) were analysed for the effect of group (WT vs. SLC6A15 KO). For the full proteome analysis, p value distributions were visualized, indicating a signal for the effect of group. Given that the whole proteome analysis is exploratory and within a small sample, we used a nominal p-value cutoff $<.05$, and report these top effects of SLC6A15 KO on the hippocampal proteome, although we additionally report the Benjamini-Hochberg false discovery rate.

We then performed a gene-annotation enrichment analysis in DAVID (Database for Annotation, Visualization and Integrated Discovery) 6.8 (Dennis et al., 2003) using differentially expressed genes in KO versus WT mice with a nominal p-value smaller than .05 and the *mus musculus* background.

2.3 | Primary cell culture

Hippocampal neurons were generated from E15-16 pups using a standard primary neuron cell culture protocol. All materials were purchased from Thermo Fisher Scientific, unless stated otherwise. Briefly, dissected hippocampi were harvested in ice-cold dissection medium (HBSS, 7 mM HEPES, 2 mM L-glutamine, 500 U/ml penicillin-streptomycin, all

Gibco®, Thermo Fisher Scientific) and dissociated using 0.25% Trypsin-EDTA (Gibco®) in a humidified incubator at 37°C and 5% CO_2. Cells were washed with serum medium (DMEM, 1% FBS, Gibco®), collected in growth medium (Neurobasal A medium, 1× B27 supplement, 0.25× GlutaMAX, all Gibco®) and seeded on clear Nunclon™ Delta 24-well plates with coverslips (12 mm, Menzel), Seahorse XF96 plates (Agilent) or black Nunclon™ 96-well plates with optical bottom. All plates/coverslips were subsequently coated overnight with 0.05 mg/ml poly-D-lysine in 0.15M borate buffer (pH = 8.4) and for 3–6 hr with 0.5–2 μg/ml laminin (Sigma Aldrich). Cells were seeded in 24-well plates at a density of 6×10^4 cells in 1 ml growth medium, in XF96 plates at 1.2×10^4 cells in 150 μl growth medium or in 96-well plates at 1.2×10^4 cells in 200 μl growth medium. Only the 60 inner wells of a 96-well plate were used for experiments, the wells of the outer rim were filled with water. All cultures were kept in a humidified incubator at 37°C and 5% CO_2.

2.4 | Electrophysiology

AMPA receptor-mediated miniature excitatory postsynaptic currents (mEPSCs) in cultured hippocampal neurons (older than D17) were recorded at room temperature (23–25°C) using an EPC9 amplifier (HEKA Electronic; Cuboni et al., 2014). Cells were continuously superfused with an extracellular solution (saturated with carbogen gas (95% O_2/5% CO_2), 2–3 ml/min flow rate) containing (in mM): 125 NaCl, 2.5 KCl, 25 $NaHCO_3$, 1.25 NaH_2PO_4, 2 $CaCl_2$, 1 $MgCl_2$, 25 D-glucose, 0.001 TTX, 0.05 APV, and 0.02 bicuculline methiodide (pH 7.4). The patch pipettes (4–6 MΩ open-tip resistance) were pulled from borosilicate glass capillaries and filled with a solution consisting of (in mM): 125 $CsCH_3SO_3$, 10 HEPES, 0.5 EGTA, 8 NaCl, 10 phosphocreatine, 4 Mg-ATP, and 0.3 GTP (pH 7.4, all potentials were corrected for a liquid junction potential of 10 mV). Visually guided somatic whole-cell voltage-clamp measurements (>1 GΩ seal resistance, <20 MΩ series resistance) were performed at −70 mV and mEPSCs were recorded 5 min after "break in" into the cell for 5 min. Recording data were low-pass filtered at 1.3 kHz and digitized at 6.5 kHz. Off-line analysis of mEPSCs was conducted using the Mini Analysis Program (Synaptosoft).

2.5 | Plate-based respirometry (seahorse technology)

To capture differences of mitochondrial respiration between WT and SLC6A15-KO neurons, oxygen consumption was measured in intact D17-21 primary hippocampal neurons

seeded at 1.5×10^4 cells per well in a Seahorse XF96-well microplate using the Seahorse XF96 Analyser (Agilent). Cells were washed with 100 µl Seahorse XF base medium (Agilent) per well and the assay was performed in 180 µl of Seahorse XF base medium. The previously water-filled rim wells were used as blanks.

Oxygen consumption rate (OCR) was measured under basal condition in Seahorse XF base medium containing 25 mM glucose and after injection of compounds interacting with the mitochondrial oxidative phosphorylation machinery. Compounds were injected as described in Figure S1. Briefly, ATP synthase was inhibited by 1 µg/ml of oligomycin (Sigma-Aldrich) to assess ATP-associated respiration. The mitochondrial proton gradient was uncoupled from ATP production by addition of the ionophore 2,4-Dinitrophenol (DNP, Sigma-Aldrich) (100 µM) in order to induce maximal respiration and calculate spare respiratory capacity. Finally, mitochondrial respiration was completely inhibited by addition of 2 µM rotenone and 2 µM antimycin A (both Sigma-Aldrich) to assess non-mitochondrial respiration and subtract it from the total measured OCR.

In order to assess if the availability of SLC6A15-substrates proline and leucine has any acute effects on respiration in WT compared to KO cells, OCR was measured in Seahorse XF base medium without glucose or pyruvate before and after injection of 0.07 mM proline or 0.80 mM leucine, respectively. The doses for proline and leucine were based on the respective concentrations in the Neurobasal A growth medium, in which the cells where grown.

2.6 | ATP

ATP content was measured in WT and KO primary hippocampal neurons seeded at 1.4×10^4 cells per well using the Promega CellTiter-Glo® Kit (Promega) according to the manufacturer's instruction with an integration time of 1 min. Only the inner 60 wells were seeded with cells, the wells of the outer rim were filled with water and some of them were used as blanks.

2.7 | Glutathione

GSH and GSSG, the reduced and oxidized form of glutathione, were measured using the GSH/GSSG-Glo™ Assay (Promega) on D18 in primary hippocampal cells seeded at 1.3×10^4 as described above in a black 96-well plates (Thermofisher). The assay was performed according to the manufacturer's instructions. GSSG and GSH were measured in separate wells. Only the inner 60 wells were seeded with cells, the wells of the outer rim were filled with water and some of them were used as blanks.

2.8 | Neurite outgrowth

Neurite outgrowth was assessed on D7, D14 and D21 using the neurite outgrowth staining kit (Invitrogen™, CA, USA) in primary hippocampal cells seeded at 1.3×10^4 (as described above) in a black 96-well optical-bottom plate with polymer base. Only the inner 60 wells were seeded with cells, the wells of the outer rim were filled with water and used as blanks. The assay was performed according to the manufacturer's instructions. Briefly, growth medium was removed and both cells and blank wells were incubated for 20 min with staining solution containing 1M PBS and 0.1% of both the cell membrane and the cell viability dye. The staining solution was then replaced by the background suppression solution containing 1M PBS and 1% background suppression dye and fluorescence was measured subsequently using a Citation3 plate reader (BioTek) at excitation 485 nm, emission 528 nm for cell viability stain and excitation 530 nm, emission 590 nm for cell membrane stain. Neurite outgrowth was quantified by dividing the blanked emission value for the cell membrane stain by the blanked one for the cell viability stain.

2.9 | Statistical analysis

Statistical analyses were calculated using IBM PASW Statistics 18 (IBM). Data were tested for normal distribution using the Kolmogorov–Smirnov test and variance homogeneity using Levene's test for homogeneity of variance. We used an independent sample t-test for data that met criteria for normal distribution and variance homogeneity and the Mann–Whitney U test for data that did not. Graphs were created using GraphPad PRISM 8 (GraphPad Software, Inc.). Bars represent the arithmetic mean with SEM (standard error of the mean); significance was set at $p < .05$.

3 | RESULTS

3.1 | Proteomics

Our proteomics analysis identified 5,996 expressed proteins, of which 81 were differently expressed in hippocampal tissue homogenates of KO compared to WT mice (Table S1, $p < .05$). Interestingly, the majority (70 proteins) were found to be downregulated in KO animals (Figure 1a,b). SLC6A15 was not detected in either WT or KO tissue, likely due to comparably low overall expression levels. STRING v11.0 analysis (Szklarczyk et al., 2019) showed that our network of 81 differently expressed proteins has significantly more interactions than expected (36 found, 26 expected, $p = .0316$, network Figure 1c). We then used DAVID 6.8 on our list of

81 proteins to identify pathways and processes affected by the lack of SLC6A15 in the hippocampus. Table S2 shows an overview of identified enriched pathways and gene ontology (GO) terms. The top enriched KEGG pathways were adherens junctions and metabolic pathways. In the section of GO Biological process, terms regarding hippocampus and cortex
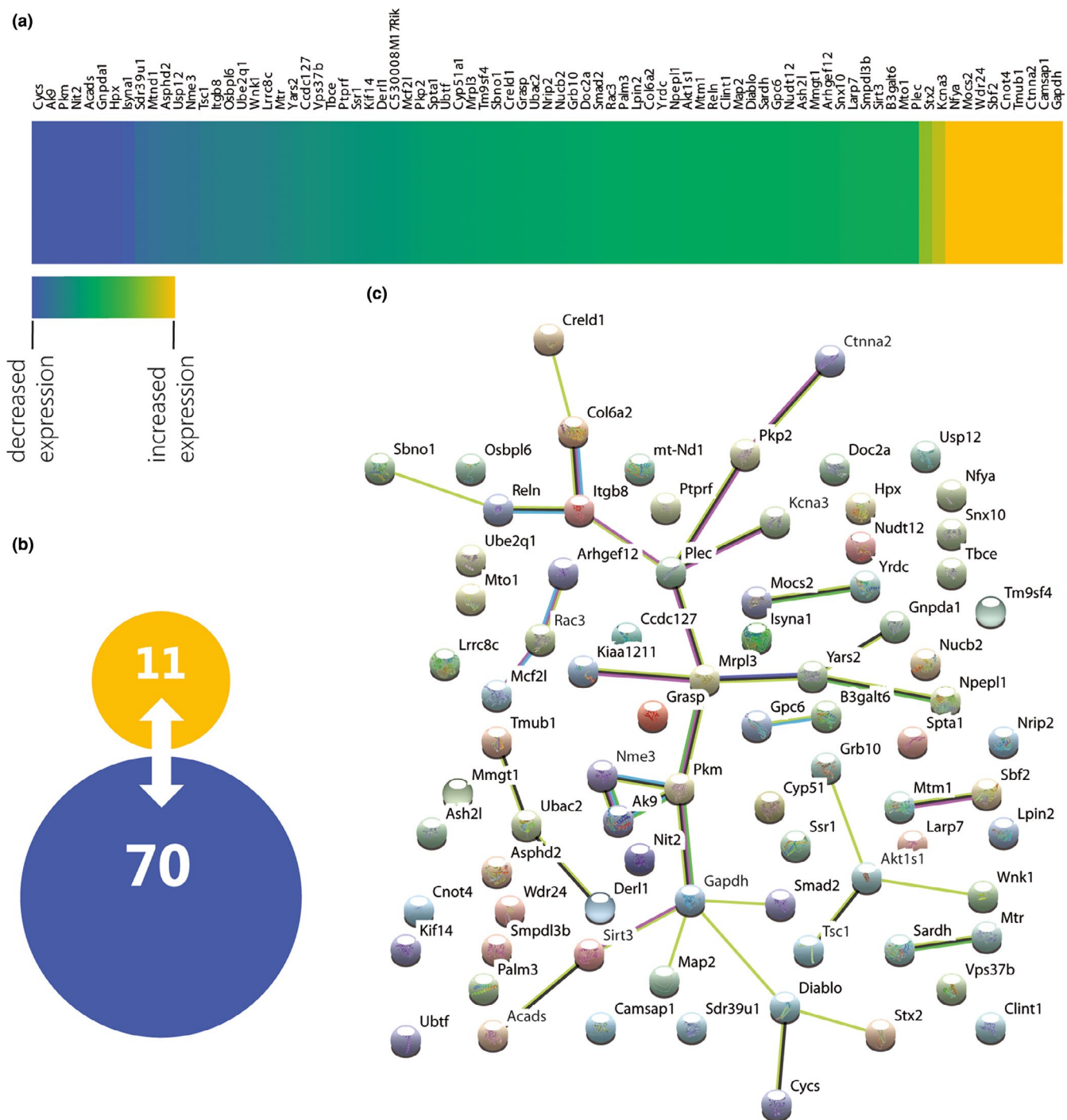

FIGURE 1 *Slc6a15*-KO affected protein expression in the proteomics analysis of the dorsal hippocampus of WT and Slc6a15-KO mice. (a) Regulated proteins with a cut-off of *p* < .05 are sorted from the ones with the most significant decrease in expression on the left to the most significant upregulated proteins on the right. (b) In total, 11 proteins were found to be upregulated and 70 proteins were downregulated. (c) STRING analysis of the 81 regulated proteins. Colour code: Edges represent associations between proteins, which are not necessarily of physical nature, but indicate a contribution of those proteins to a shared function. Known interactions: Turquoise = from curated databases, magenta = experimentally determined. Predicted interactions: Gras green = gene neighbourhood, red = gene fusions, bright blue = gene co-occurrence. Others: lime = textmining, black = co-expression, lavender = protein homology
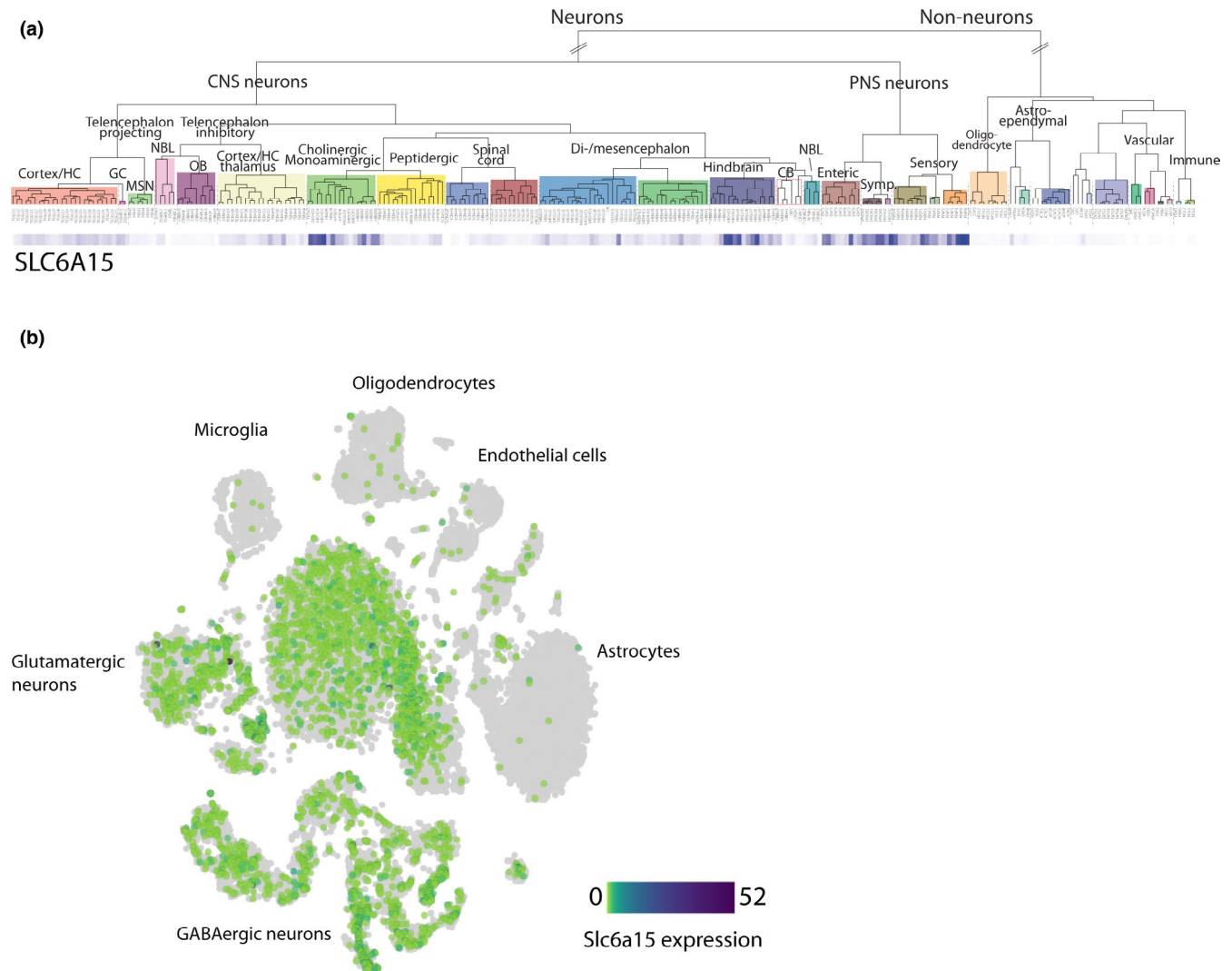
(a)

(b)

FIGURE 2 Gene expression of *Slc6a15* in different cell types. (a) Expression of *Slc6a15* across different cell types. The heat map at the bottom indicates the detected strength of *Slc6a15* expression, with darker colours indicating stronger expression (b) Scatter plot of Slc6a15 expression across 18,147 hippocampal cells labelled for different cell types

development as well as negative regulation of insulin receptor signalling, TOR signalling and cell size were enriched. Equally interesting, the category GO Cellular compartment yielded apart from the rather general cytoplasm and cytoskeleton also lamellipodium and cell-cell adherens junction as well as mitochondrion and mitochondrial matrix. While the results from the proteomics analysis are exploratory and would need to be validated in replication studies for individual proteins and pathways, they were used as guidance for a following more in-depth analysis of biological processes.

3.2 | Single cell expression of Slc6a15 in hippocampus

Next, since very little is known about cell-type specificity of *Slc6a15* in the mouse brain, we explored its expression using publicly available single-cell RNA sequencing data from 18,147

mouse hippocampal cells (Zeisel et al., 2015). Interestingly, we detected in the central nervous system an enrichment of *SLC6A15* expression in the hippocampus, but also on cholinergic/monoaminergic nuclei of the hindbrain (Figure 2a). Furthermore, *Slc6a15* was found to be mostly expressed in glutamatergic and GABAergic neurons (Figure 2b). When investigating the expression of the 81 differentially expressed proteins from the proteomics analysis in this data set, we could confirm that there is a high level of expression of these transcripts in the mouse hippocampus (Figure S1). Based on the proteomics and single-cell data, we decided to follow upon metabolic and glutamatergic function in neurons.

3.3 | Electrophysiology

AMPA receptor-mediated mEPSCs in mature primary hippocampal neurons (older than D17) were recorded using

the whole-cell patch-clamp technique. Figure 3a–c shows the effect of *Slc6a15*-KO on mEPSC frequency and amplitude. *Slc6a15*-KO significantly decreased mEPSC frequency ($U = 66$, $p = .0002$), but not amplitude ($U = 148$, $p = .2$).

3.4 | Respirometry and ATP

Next, we assessed different aspects of cellular respiration by measuring the oxygen consumption rate (OCR) in intact primary neurons. Basal, ATP-coupled and maximal respiration were increased in KO cells when compared to WT cells in the standard XF base medium in the presence of 25 mM glucose (basal respiration: $F = 10.46$, $p = .0039$; ATP-coupled respiration: $F = 8.59$, $p = .0079$; maximal respiration: $F = 26.3$, $p = .00004$; Figure 4a–c). Spare respiratory capacity, determined as maximal respiration minus basal respiration OCR, was also increased in KO cells ($F = 38.07$, $p = 4 \times 10^{-6}$, Figure 4d). Cellular respiratory control ($F = 6.03$, $p = .023$, Figure 4e) was increased while coupling efficiency, determining the respiratory fraction dedicated to ATP production (fraction of ATP production-coupled OCR of basal OCR) was not ($F = 3.97$, $p = .059$, Figure 4f). The OCR experimental trace over time can be seen in the Figure S2. We asked whether the observed increase in respiration in KO cells was due to any direct effects of the (missing) SLC6A15 substrates or an inherent attribute of the KO cells. Therefore, we tested the cells in the same XF base medium without glucose and injected either proline or leucine, respectively. The acute administration of proline or leucine did not impose acute effects on basal respiration, neither in WT nor KO cells (2-way-ANOVA, $p = .86$ for substrate injection, Figure 4g). Increased ATP turnover observed in respiratory

measurements was corroborated in a separate independent experiment using a luminescent cell viability assay, confirming increased ATP levels in *Slc6a15*-KO cells ($F = 4.03$, $p = .033$; Figure 4h).

3.5 | Glutathione

In order to assess the consequences of *Slc6a15*-KO on the redox-state of the cells, we measured total levels of glutathione (GSH and GSSG) and its oxidized form, GSSG. While KO cells had increased levels of both total glutathione (GSH and GSSG; $U = 1$, $p = .0003$) and GSSG ($U = 4$, $p = .0008$; Figure 5a,b), they also had a lower percentage of GSSG to total glutathione ($U = 2$, $p = .0003$; Figure 5c), indicating a higher proportion of the reduced GSH.

3.6 | Neurite outgrowth

Finally, we performed a neurite outgrowth assay on D8, 13 and 17 in *Slc6a15*-KO and WT cells. We found that KO cells showed an increased membrane stain ($F_{1,58} = 24.2$, $p < .0001$; Figure 6a), viability stain ($F_{1,116} = 57.9$, $p < .0001$; Figure 6b) and ratio of membrane to viability stain ($F_{1,58} = 56.6$, $p < .0001$; Figure 6c), indicating a faster growth in the KO neurons.

4 | DISCUSSION

Several studies have associated SLC6A15 with different aspects of psychiatric disorders, for example with an
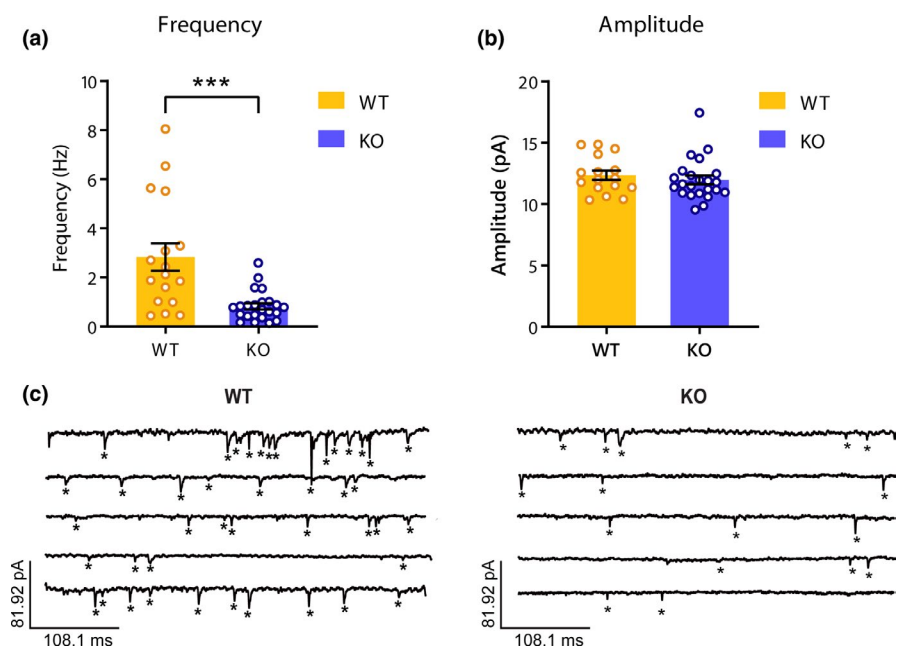

FIGURE 3 *Slc6a15*-KO decreases miniature excitatory postsynaptic current (mEPSC) frequency but not amplitude in primary hippocampal neurons. Summary of the effect of *Slc6a15*-KO on mEPSC frequency (a) and amplitude (b). Representative traces from 5 different WT and KO cells are shown in (c). *n* (number of recorded cells, WT) = 17; *n* (KO) = 23. $p^{***} < .001$, bars represent mean ± *SEM*
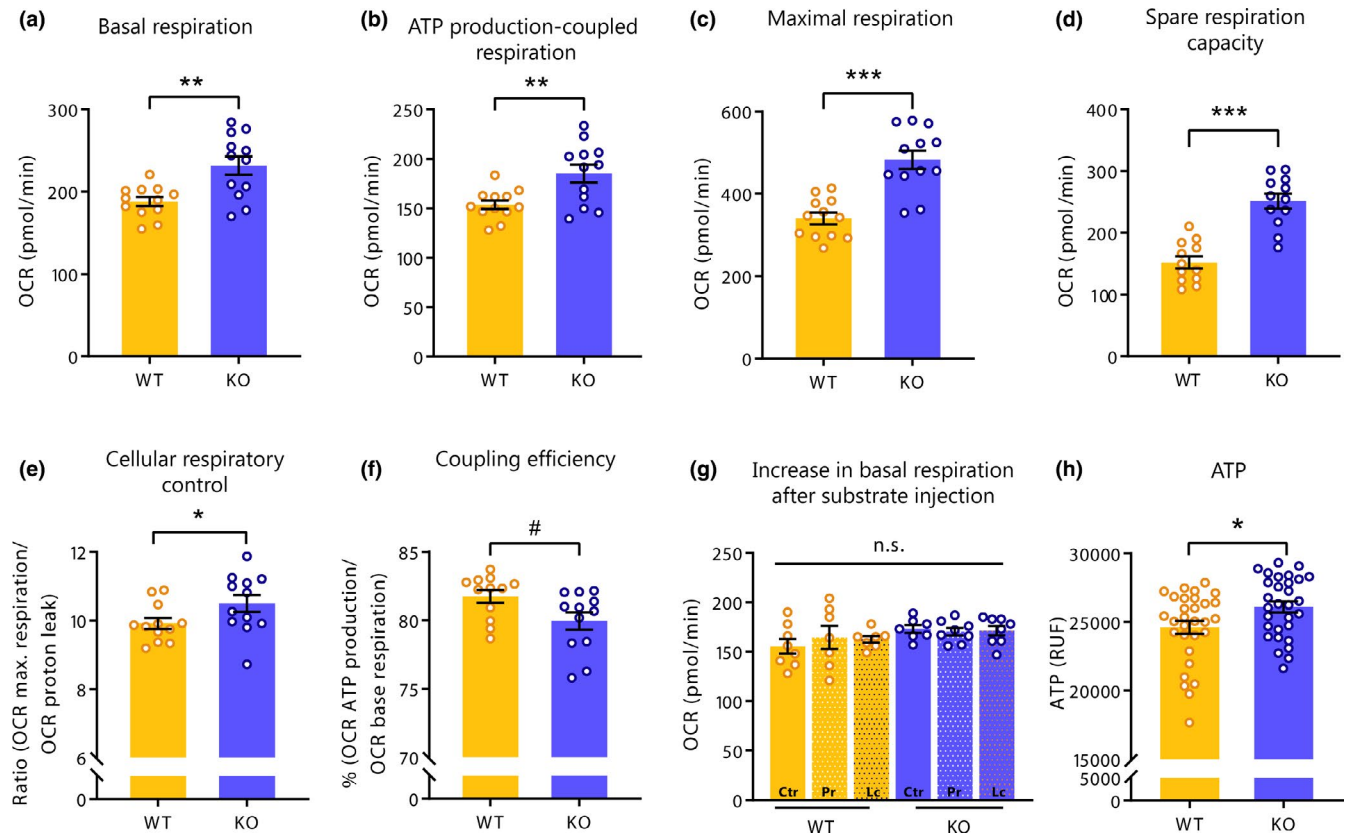
FIGURE 4 *Slc6a15*-KO increased several aspects of cellular respiration assessed by measuring the oxygen consumption rate (OCR) in primary hippocampal neurons. (a) Basal respiration (b) ATP-coupled respiration (c) maximal respiration (d) spare respiratory capacity (=maximal respiration minus basal respiration OCR) (e) cellular respiratory control (=maximal respiration/ proton leak) (f) coupling efficiency (=ratio of ATP production-coupled OCR to base respiration OCR). (g) Injection of proline or leucine at baseline without glucose or pyruvate did not affect basal respiration. (h) *Slc6a15*-KO increased ATP levels in a separate measurement. n (number of wells) = 12 for a–f; n = 7–8 for g; n = 30 for h. Bars represent mean ± *SEM*. *$p < .05$, **$p < .01$, ***$p < .001$ and #$p < .1$
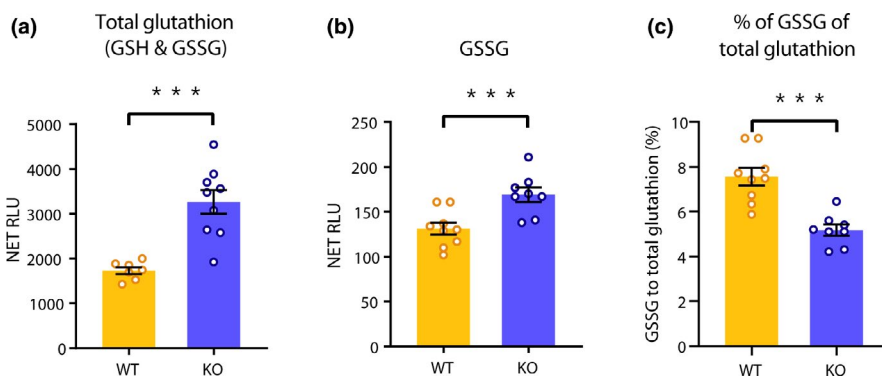

FIGURE 5 *Slc6a15*-KO increased levels of total glutathione (a) and of the total amount of oxidized form (GSSG) (b), but reduced the percentage of GSSG to total glutathione (c). Bars represent mean ± *SEM*. n (number of wells, WT) = 7–9, n (KO) = 7–8. ***$p < .001$

increased risk of MDD and difficulties in regulating the HPA axis (Kohli et al., 2011; Schuhmacher et al., 2013). In addition, animal studies indicate that this neutral amino acid transporter affects stress resilience phenotypes (Chandra et al., 2017; Santarelli et al., 2016). However, the cellular mechanisms that SLC6A15 controls and how they may lead to the association with psychiatric disorders and stress resilience are not yet understood. Here, we present the first evidence that lack of SLC6A15 affects a number of prominent neuronal functions, including glutamatergic neurotransmission, mitochondrial function and neuronal growth.

4.1 | Lack of SLC6A15 affects the hippocampal proteome

To gain insight into the potential cellular functions affected by SLC6A15, we first performed a proteomics analysis on
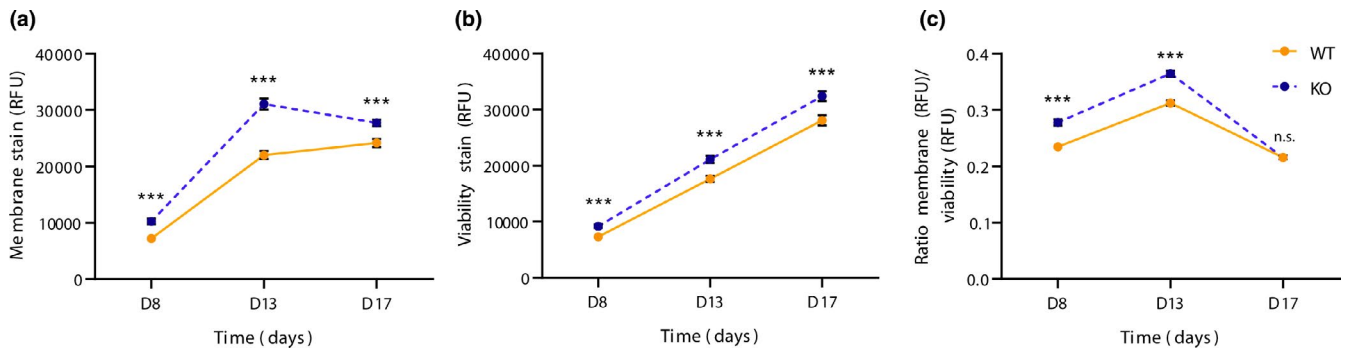
FIGURE 6 *Slc6a15*-KO increased neurite outgrowth in primary hippocampal neurons after 8 and 13 days in culture. (a) membrane stain, (b) viability stain, (c) ratio of membrane and viability stain. Points represent mean ± *SEM*. *n* (number of wells, WT) = 29–30, *n* (KO) = 29–30. ****p* < .001, n.s. = not significant

the hippocampus and identified a moderate number of differentially expressed proteins, most of which were decreased in expression in *Slc6a15*-KO mice. Interestingly, the observed proteins form a regulatory network and the pathway analysis indicated a number of interesting cellular domains that were affected, including metabolic, structural and mitochondrial functions. For example, the most significantly regulated protein, Catenin alpha 2 (CTNNA2) controls synaptic spine stability and synaptic contacts (Abe et al., 2004). Another interesting candidate protein found to be differentially expressed is Monoamine oxidase A (MAO-A), which is attached to the outer mitochondrial membrane (Bortolato & Shih, 2011) and has previously been heavily implicated in a number of psychiatric disorders, including MDD (Hamon & Blier, 2013; Mandelli & Serretti, 2013). It should be noted, though, that the proteomics analysis was exploratory in nature and the differentially expressed proteins need to be validated in future studies. Following confirmation that SLC6A15 is indeed primarily expressed in neurons, we next focused on neuronal activity, cellular metabolism and mitochondrial function as potentially affected phenotypes in SLC6A15 KO cells.

4.2 | SLC6A15 knockout leads to reduced frequency of AMPA-mediated mEPSCs

As previous reports on SLC6A15 already speculated that glutamatergic signalling might be affected by this transporter (Kohli et al., 2011) and especially glutamate tissue concentration was found to be reduced in the hippocampus of SLC6A15 KO mice (Santarelli et al., 2015), we hypothesized that neuronal activity might directly be affected. Indeed, our results demonstrate that the spontaneous release probability of excitatory neurons is significantly reduced in SLC6A15 KO cells. Given that high glutamate levels are neurotoxic (Olloquequi et al., 2018) and the established link between glutamate neurotransmission and psychiatric disorders such as MDD (Duman et al., 2019), it is possible that a reduction in SLC6A15 expression could lead to reduced neuronal activity, which would be

neuroprotective and pro-resilient especially under high demand conditions. Indeed supporting this hypothesis, SLC6A15 KO mice are resilient to chronic social stress exposure (Santarelli et al., 2016). In future studies it would be interesting to test whether SLC6A15 can also alter stimulated release of glutamate in vitro and in vivo, which would further support its role in modulating glutamate signalling.

4.3 | SLC6A15 deletion enhances mitochondrial function and cellular metabolism

The role of glutamatergic signalling in neuropsychiatric disorders is tightly linked to neuroinflammation and specifically the function of mitochondria (Réus et al., 2015). For example, hereditary mitochondrial disorders were previously found to be associated to a high degree with psychiatric disorders (Morava & Kozicz, 2013; Preston et al., 2018). There is also mounting evidence indicating that mitochondrial function and spare respiratory capacity might contribute to mechanisms of plasticity and stress resilience (Cherix et al., 2020; Choi et al., 2009; Filiou & Sandi, 2019; Papilloud et al., 2018; Picard et al., 2018). This is of central importance given the close connection of SLC6A15 with stress and stress-related psychopathologies (Kohli et al., 2011; Santarelli et al., 2016) and further points to a decisive role of altered mitochondrial function in stress-related disorders.

Next to their well-known role in producing ATP via oxidative phosphorylation, mitochondria play a key function in the brain with their ability to modulate Ca^{2+} concentrations and central control in glutamate synthesis (Nunnari & Suomalainen, 2012). It is therefore intriguing that deletion of SLC6A15 causes increased mitochondrial function and – in line with this observation – an increased GSH/GSSG redox ratio. A low glutathione redox ratio in the brain has been repeatedly observed in a number of neuropsychiatric disorders (Gu et al., 2015) and ways to increase GSH levels would be promising avenues for novel treatments of psychiatric

disorders (Morris et al., 2014). Whether or not the observed effects on mitochondrial function by SLC6A15 are causally related to the altered uptake of neutral amino acids remains to be shown, as a replacement of glucose with proline or leucine did not alter mitochondrial respiration. One possible explanation for this could be that the doses used for proline or leucine were too low to observe an effect.

4.4 | SLC6A15 knockout promotes neurite outgrowth

Mitochondria play important roles in controlling fundamental functions in neuroplasticity, including neurite outgrowth (Cheng et al., 2010). In line with this, we observed a significant increase in neurite outgrowth in primary neurons lacking SLC6A15. Such a phenotype would be expected from increased mitochondrial function. Importantly, psychiatric disorders are associated with hippocampal atrophy and reduced connectivity (Duman et al., 2019), and antidepressant treatment reverses this deficit (Banasr et al., 2011).

5 | CONCLUSION

Taken together, our results highlight the potentially important contribution of the neutral amino acid transporter SLC6A15 in modulating brain functions, with direct implications for psychiatric disorders, such as MDD. We propose that by controlling intracellular concentrations of neutral amino acids like proline, this transporter affects mitochondrial activity. In addition, the alterations in spontaneous release probability of excitatory neurons could be related to altered intracellular glutamate levels due to changes in proline-dependent glutamate synthesis. Finally, both the changes in mitochondrial function as well as release probability of glutamate could contribute to the observed morphological and structural changes of SLC6A15 KO cells, which may also underlie the previously observed behavioural phenotype of SLC6A15 KO mice. It will be interesting to test if SLC6A15 deletion in mice or SLC6A15 polymorphisms in humans can lead to altered hippocampal volumes or dendritic structures. Overall these data provide further indications that a pharmacological or genetic reduction of SLC6A15 activity may represent a promising approach for a novel antidepressant therapy.

CONFLICT OF INTEREST
The authors declare no conflict of interest.

AUTHOR CONTRIBUTIONS
KS and MVS conceived the study. KS performed the experiments and analyses. OK and ME performed the electrophysiological recordings and analysis. DL and MJ assisted with the performance and analysis of the mitochondrial bioenergetics. FH and AC contributed to the study design and data interpretation. NCG, SM and NN performed and analysed the proteomics analysis. JPL provided the single cell transcriptomics analysis and data interpretation. KS and MVS wrote the initial draft of the manuscript. All authors contributed to the revision of the manuscript.

DATA AVAILABILITY STATEMENT
All raw data are available upon request.

PEER REVIEW
The peer review history for this article is available at https://publons.com/publon/10.1111/ejn.14990.

ORCID
Alon Chen https://orcid.org/0000-0003-3625-8233
Mathias V. Schmidt https://orcid.org/0000-0002-3788-2268

REFERENCES

Abe, K., Chisaka, O., van Roy, F., & Takeichi, M. (2004). Stability of dendritic spines and synaptic contacts is controlled by αN-catenin. *Nature Neuroscience*, 7, 357–363.

Banasr, M., Dwyer, J. M., & Duman, R. S. (2011). Cell atrophy and loss in depression: Reversal by antidepressant treatment. *Current Opinion in Cell Biology*, 23, 730–737.

Bortolato, M., & Shih, J. C. (2011). Behavioral outcomes of monoamine oxidase deficiency: Preclinical and clinical evidence. *International Review of Neurobiology*, 100, 13–42.

Chandra, R., Francis, T. C., Nam, H., Riggs, L. M., Engeln, M., Rudzinskas, S., Konkalmatt, P., Russo, S. J., Turecki, G., Iniguez, S. D., & Lobo, M. K. (2017). Reduced Slc6a15 in nucleus accumbens D2-neurons underlies stress susceptibility. *The Journal of Neuroscience.*, 37, 6527–6538.

Cheng, A., Hou, Y., & Mattson, M. P. (2010). Mitochondria and neuroplasticity. *ASN Neuro*, 2, e00045. https://doi.org/10.1042/AN20100019

Cherix, Antoine, Larrieu, Thomas, Grosse, Jocelyn, Rodrigues, João, McEwen, Bruce, Nasca, Carla, Gruetter, Rolf, & Sandi, Carmen (2020). Metabolic signature in nucleus accumbens for anti-depressant-like effects of acetyl-L-carnitine. *eLife*, 9. https://doi.org/10.7554/eLife.50631

Choi, S. W., Gerencser, A. A., & Nicholls, D. G. (2009). Bioenergetic analysis of isolated cerebrocortical nerve terminals on a microgram scale: Spare respiratory capacity and stochastic mitochondrial failure. *Journal of Neurochemistry*, *109*, 1179–1191. https://doi.org/10.1111/j.1471-4159.2009.06055.x

Cox, J., Hein, M. Y., Luber, C. A., Paron, I., Nagaraj, N., & Mann, M. (2014). Accurate proteome-wide label-free quantification by delayed normalization and maximal peptide ratio extraction, termed MaxLFQ. *Molecular & Cellular Proteomics*, *13*, 2513–2526. https://doi.org/10.1074/mcp.M113.031591

Cox, J., & Mann, M. (2008). MaxQuant enables high peptide identification rates, individualized p.p.b.-range mass accuracies and proteome-wide protein quantification. *Nature Biotechnology*, *26*, 1367–1372.

Cuboni, S., Devigny, C., Hoogeland, B., Strasser, A., Pomplun, S., Hauger, B., Höfner, G., Wanner, K. T., Eder, M., Buschauer, A., Holsboer, F., & Hausch, F. (2014). Loratadine and analogues: Discovery and preliminary structure-activity relationship of inhibitors of the amino acid transporter B(0)AT2. *Journal of Medicinal Chemistry*, *57*, 9473–9479.

Dennis, G., Sherman, B. T., Hosack, D. A., Yang, J., Gao, W., Lane, H. C., & Lempicki, R. A. (2003). DAVID: Database for annotation, visualization, and integrated discovery. *Genome Biology*, *4*, P3.

Drgonova, J., Liu, Q.-R., Hall, F. S., Krieger, R. M., & Uhl, G. R. (2007). Deletion of v7–3 (SLC6A15) transporter allows assessment of its roles in synaptosomal proline uptake, leucine uptake and behaviors. *Brain Research*, *1183*, 10–20.

Duman, R. S., Sanacora, G., & Krystal, J. H. (2019). Altered connectivity in depression: GABA and glutamate neurotransmitter deficits and reversal by novel treatments. *Neuron*, *102*, 75–90. https://doi.org/10.1016/j.neuron.2019.03.013

Farmer, M. K., Robbins, M. J., Medhurst, A. D., Campbell, D. A., Ellington, K., Duckworth, M., Brown, A. M., Middlemiss, D. N., Price, G. W., & Pangalos, M. N. (2000). Cloning and characterization of human NTT5 and v7–3: Two orphan transporters of the Na$^+$/Cl$^-$-dependent neurotransmitter transporter gene family. *Genomics*, *70*, 241–252. https://doi.org/10.1006/geno.2000.6387

Filiou, M. D., & Sandi, C. (2019). Anxiety and brain mitochondria: A bidirectional crosstalk. *Trends in Neurosciences*, *42*, 573–588.

Gu, F., Chauhan, V., & Chauhan, A. (2015). Glutathione redox imbalance in brain disorders. *Current Opinion in Clinical Nutrition and Metabolic Care*, *18*, 89–95.

Hamon, M., & Blier, P. (2013). Monoamine neurocircuitry in depression and strategies for new treatments. *Progress in Neuro-Psychopharmacology and Biological Psychiatry*, *45*, 54–63.

Hyde, C. L., Nagle, M. W., Tian, C., Chen, X., Paciga, S. A., Wendland, J. R., Tung, J. Y., Hinds, D. A., Perlis, R. H., & Winslow, A. R. (2016). Identification of 15 genetic loci associated with risk of major depression in individuals of European descent. *Nature Genetics*, *48*, 1031–1036.

Inoue, K., Sato, K., Tohyama, M., Shimada, S., & Uhl, G. R. (1996). Widespread brain distribution of mRNA encoding the orphan neurotransmitter transporter v7–3. *Molecular Brain Research*, *37*, 217–223.

James, S. L., Abate, D., Abate, K. H., Abay, S. M., Abbafati, C., Abbasi, N., Abbastabar, H., Abd-Allah, F., Abdela, J., Abdelalim, A., Abdollahpour, I., Abdulkader, R. S., Abebe, Z., Abera, S. F., Abil, O. Z., Abraha, H. N., Abu-Raddad, L. J., Abu-Rmeileh, N. M. E., Accrombessi, M. M. K., … Murray, C. J. L. (2018). Global, regional, and national incidence, prevalence, and years lived with disability for 354 diseases and injuries for 195 countries and territories, 1990–2017: A systematic analysis for the Global Burden of Disease Study 2017. *The Lancet*, *392*, 1789–1858. https://doi.org/10.1016/S0140-6736(18)32279-7

Kohli, M. A., Lucae, S., Saemann, P. G., Schmidt, M. V., Demirkan, A., Hek, K., Czamara, D., Alexander, M., Salyakina, D., Ripke, S., Hoehn, D., Specht, M., Menke, A., Hennings, J., Heck, A., Wolf, C., Ising, M., Schreiber, S., Czisch, M., … Binder, E. B. (2011). The neuronal transporter gene SLC6A15 confers risk to major depression. *Neuron*, *70*, 252–265. https://doi.org/10.1016/j.neuron.2011.04.005

Mandelli, L., & Serretti, A. (2013). Gene environment interaction studies in depression and suicidal behavior: An update. *Neuroscience and Biobehavioral Reviews*, *37*, 2375–2397.

Morava, E., & Kozicz, T. (2013). Mitochondria and the economy of stress (mal)adaptation. *Neuroscience and Biobehavioral Reviews*, *37*, 668–680.

Morris, G., Anderson, G., Dean, O., Berk, M., Galecki, P., Martin-Subero, M., & Maes, M. (2014). The glutathione system: A new drug target in neuroimmune disorders. *Molecular Neurobiology*, *50*, 1059–1084.

Nagaraj, N., Kulak, N. A., Cox, J., Neuhauser, N., Mayr, K., Hoerning, O., Vorm, O., & Mann, M. (2012). System-wide perturbation analysis with nearly complete coverage of the yeast proteome by single-shot ultra HPLC runs on a bench top Orbitrap. *Molecular & Cellular Proteomics*, *11*(M111), 013722. https://doi.org/10.1074/mcp.M111.013722

Nunnari, J., & Suomalainen, A. (2012). Mitochondria: In sickness and in Health. *Cell*, *148*, 1145–1159. https://doi.org/10.1016/j.cell.2012.02.035

O'Mara, M., Oakley, A., & Bröer, S. (2006). Mechanism and putative structure of B(0)-like neutral amino acid transporters. *Journal of Membrane Biology*, *213*, 111–118.

Olloquequi, J., Cornejo-Córdova, E., Verdaguer, E., Soriano, F. X., Binvignat, O., Auladell, C., & Camins, A. (2018). Excitotoxicity in the pathogenesis of neurological and psychiatric disorders: Therapeutic implications. *Journal of Psychopharmacology*, *32*, 265–275.

Papilloud, A., Guillot de Suduiraut, I., Zanoletti, O., Grosse, J., & Sandi, C. (2018). Peripubertal stress increases play fighting at adolescence and modulates nucleus accumbens CB1 receptor expression and mitochondrial function in the amygdala. *Translational Psychiatry*, *8*, 156.

Picard, M., McEwen, B. S., Epel, E. S., & Sandi, C. (2018). An energetic view of stress: Focus on mitochondria. *Frontiers in Neuroendocrinology*, *49*, 72–85.

Preston, G., Kirdar, F., & Kozicz, T. (2018). The role of suboptimal mitochondrial function in vulnerability to post-traumatic stress disorder. *Journal of Inherited Metabolic Disease*, *41*, 585–596.

Rappsilber, J., Ishihama, Y., & Mann, M. (2003). Stop and go extraction tips for matrix-assisted laser desorption/ionization, nanoelectrospray, and LC/MS sample pretreatment in proteomics. *Analytical Chemistry*, *75*, 663–670.

Réus, G. Z., Fries, G. R., Stertz, L., Badawy, M., Passos, I. C., Barichello, T., Kapczinski, F., & Quevedo, J. (2015). The role of inflammation and microglial activation in the pathophysiology of psychiatric disorders. *Neuroscience*, *300*, 141–154. https://doi.org/10.1016/j.neuroscience.2015.05.018

Santarelli, S., Namendorf, C., Anderzhanova, E., Gerlach, T., Bedenk, B., Kaltwasser, S., Wagner, K., Labermaier, C., Reichel, J., Drgonova, J., Czisch, M., Uhr, M., & Schmidt, M. V. (2015). The amino acid

transporter SLC6A15 is a regulator of hippocampal neurochemistry and behavior. *Journal of Psychiatric Research*, *68*, 261–269.

Santarelli, S., Wagner, K. V., Labermaier, C., Uribe, A., Dournes, C., Balsevich, G., Hartmann, J., Masana, M., Holsboer, F., Chen, A., Müller, M. B., & Schmidt, M. V. (2016). SLC6A15, a novel stress vulnerability candidate, modulates anxiety and depressive-like behavior: Involvement of the glutamatergic system. *Stress*, *19*, 83–90. https://doi.org/10.3109/10253890.2015.1105211

Schuhmacher, A., Lennertz, L., Wagner, M., Höfels, S., Pfeiffer, U., Guttenthaler, V., Maier, W., Zobel, A., & Mössner, R. (2013). A variant of the neuronal amino acid transporter SLC6A15 is associated with ACTH and cortisol responses and cognitive performance in unipolar depression. *International Journal of Neuropsychopharmacology*, *16*, 83–90. https://doi.org/10.1017/S1461145712000223

Schumann, G., Binder, E. B., Holte, A., de Kloet, E. R., Oedegaard, K. J., Robbins, T. W., Walker-Tilley, T. R., Brown, V. J., Buitelaar, J., Ciccocioppo, R., Cools, R., Escera, C., Fleischhacker, W., Flor, H., Frith, C. D., Heinz, A., Johnsen, E., Kirschbaum, C., Klingberg, T., … Wittchen, H. U. (2014). Stratified medicine for mental disorders. *European Neuropsychopharmacology*, *24*, 5–50.

Szklarczyk, D., Gable, A. L., Lyon, D., Junge, A., Wyder, S., Huerta-Cepas, J., Simonovic, M., Doncheva, N. T., Morris, J. H., Bork, P., Jensen, L. J., & von Mering, C. (2019). STRING v11: Protein-protein association networks with increased coverage, supporting functional discovery in genome-wide experimental datasets. *Nucleic Acids Research*, *47*, D607–D613. https://doi.org/10.1093/nar/gky1131

Takanaga, H., Mackenzie, B., Peng, J.-B., & Hediger, M. A. (2005). Characterization of a branched-chain amino-acid transporter SBAT1 (SLC6A15) that is expressed in human brain. *Biochemical and Biophysical Research Communications*, *337*, 892–900.

Wittchen, H. U., Jacobi, F., Rehm, J., Gustavsson, A., Svensson, M., Jönsson, B., Olesen, J., Allgulander, C., Alonso, J., Faravelli, C., Fratiglioni, L., Jennum, P., Lieb, R., Maercker, A., van Os, J., Preisig, M., Salvador-Carulla, L., Simon, R., & Steinhausen, H.-C. (2011). The size and burden of mental disorders and other disorders of the brain in Europe 2010. *European Neuropsychopharmacology*, *21*, 655–679.

Zeisel, A., Muñoz-Manchado, A. B., Codeluppi, S., Lönnerberg, P., La Manno, G., Juréus, A., Marques, S., Munguba, H., He, L., Betsholtz, C., Rolny, C., Castelo-Branco, G., Hjerling-Leffler, J., & Linnarsson, S. (2015). Brain structure. Cell types in the mouse cortex and hippocampus revealed by single-cell RNA-seq. *Science*, *347*, 1138–1142. https://doi.org/10.1126/science.aaa1934

SUPPORTING INFORMATION

Additional supporting information may be found online in the Supporting Information section.